Available online at www.sciencedirect.com
ScienceDirect
Earth and Planetary Science Letters 259 (2007) 442–456
EPSL
www.elsevier.com/locate/epsl

A high-resolution, absolute-dated deglacial speleothem record of Indian Ocean climate from Socotra Island, Yemen

Jeremy D. Shakun [a,*], Stephen J. Burns [a], Dominik Fleitmann [b], Jan Kramers [c], Albert Matter [b], Abdulkarim Al-Subary [d]

[a] *Department of Geosciences, Morrill Science Center, University of Massachusetts, Amherst, MA 01003, USA*
[b] *Institute of Geological Sciences, University of Bern, Bern, Switzerland*
[c] *Institute of Meteorology, University of Leipzig, Leipzig, Germany*
[d] *Department of Geological Sciences, Sana'a University, Sana'a, Yemen*

Received 18 July 2006; received in revised form 16 April 2007; accepted 3 May 2007
Available online 8 May 2007
Editor: H. Elderfield

Abstract

Stalagmite M1-5 from Socotra Island, Yemen in the northwest Indian Ocean provides a robust, high-resolution paleoclimate record from ~27.4–11.1 ka based on 717 stable isotope and 28 ^{230}Th measurements. Variations in M1-5 oxygen isotope ratios (δ^{18}O) are interpreted to be primarily driven by an amount effect related to changes in the mean position and/or intensity of convection of the intertropical convergence zone, the island's only source of precipitation. The M1-5 δ^{18}O time series is strongly correlated to the Greenland ice cores, similar to an older Socotra speleothem deposited from 53–40 ka [S.J. Burns, D. Fleitmann, A. Matter, J. Kramers, A. Al-Subbary, Indian Ocean climate and an absolute chronology over Dansgaard/Oeschger events 9 to 13, Science 301 (2003) 1365–1367], indicating that a North Atlantic–Indian Ocean cold-dry/warm-wet teleconnection persisted through the end of the last glacial period. Peak aridification occurred at ~23 ka and a gradual increase in moisture thereafter was interrupted by an abrupt drying event at ~16.4 ka, perhaps related to Heinrich event 1. Indian Ocean rainfall increased dramatically during the Bølling period and then decreased continuously and gradually through the Allerød and Younger Dryas. The Holocene began abruptly with increased precipitation at 11.4 ka and was followed by a major but short-lived drying during the Preboreal Oscillation at ~11.2 ka. M1-5 is highly correlated to the Dongge Cave record from 15.5–11 ka, suggesting much of the Indian Ocean monsoon region responded similarly to the major climate changes of the last deglaciation. The transitions into the Younger Dryas and to a lesser extent the Bølling are remarkably gradual in M1-5, as they are in all other Asian speleothem records, occurring over several centuries. These gradual transitions are in striking contrast to high-resolution records from around the North Atlantic basin where the transitions are extremely abrupt and generally occur in under a century. This spatially variable pattern of climate change is consistent with an Atlantic origin for these deglacial climate events.

Keywords: speleothem; Indian monsoon; Socotra; intertropical convergence zone (ITCZ); deglaciation; uranium-series

1. Introduction

The East African–Asian monsoon is one of the major weather systems on the planet, providing the majority of

* Corresponding author. Present address: Department of Geosciences, Oregon State University, Corvallis, OR 97331, USA. Tel.: +1 541 737 1248; fax: +1 541 737 1200.
E-mail address: shakunj@geo.oregonstate.edu (J.D. Shakun).

0012-821X/$ - see front matter © 2007 Elsevier B.V. All rights reserved.
doi:10.1016/j.epsl.2007.05.004

rainfall to many of the most densely populated areas of the world (Global Demography Project), capable of communicating climate events across the equator (Clark et al., 1999), and exerting a major control on physical and biogeochemical processes in the Indian Ocean (Hastenrath, 1994). An understanding of its past variability and relationship to climate change elsewhere is of critical importance in making accurate predictions of its evolution and effects on other parts of the climate system. Records of the monsoon over the last deglaciation (Termination I) provide valuable information on monsoon behavior during a period of major global climate change. While numerous marine cores from the Arabian Sea provide information on the monsoon over this interval, they are of relatively low-resolution, based on radiocarbon chronologies, and are generally proxies for monsoon wind-induced upwelling as opposed to precipitation (Anderson and Prell, 1993; Sirocko et al., 1993; Schulz et al., 1998; Altabet et al., 2002; Ivanochko et al., 2005). High-resolution and well-dated deglacial records in this region come exclusively from speleothem studies and are confined to northern India (Sinha et al., 2005) and eastern China (Wang et al., 2001; Dykoski et al., 2005). Thus, there is currently a need for a high-resolution climate record over the last glacial termination from the western end of the Asian monsoon domain. We present such a record based on a speleothem from Socotra Island in the northwest Indian Ocean (Fig. 1) from ~27.4–11.1 ka (all ages are reported in thousands of years before 1950 AD).

The above-mentioned records demonstrate unequivocally a strengthening of the monsoon during the last deglaciation, likely in response to increasing Northern Hemisphere insolation and changing glacial boundary conditions, which permitted greater heating of the Asian landmass (Anderson and Prell, 1993; Cohmap, 1988; Clemens et al., 1991). Superimposed on this general strengthening were abrupt, millennial-scale increases and decreases in monsoon intensity, which appear to have occurred largely in concert with northern high latitude temperature changes. Asian speleothems and Arabian Sea cores uniformly indicate the monsoon was weaker during cold intervals such as Heinrich event 1 (H1) and the Younger Dryas (YD), and stronger during the warming of the Bølling–Allerød (B–A) (Schulz et al., 1998; Altabet et al., 2002; Ivanochko et al., 2005; Sinha et al., 2005; Wang et al., 2001; Dykoski et al., 2005; Sirocko et al., 1996). This North Atlantic–Indian Ocean teleconnection appears to have acted throughout the last glacial period (Schulz et al., 1998; Altabet et al., 2002; Ivanochko et al., 2005; Wang et al., 2001; Burns et al., 2003) and persisted through the Holocene (Dykoski et al., 2005; Fleitmann et al., 2003b; Gupta et al., 2003; Wang et al., 2005). On decadal to centennial time scales, deglacial Asian monsoon intensity, as recorded by Chinese and Indian speleothems (Sinha et al., 2005; Dykoski et al., 2005), varied at frequencies similar to the Holocene $\Delta^{14}C$ record. These findings suggest a possible solar influence on the monsoon during this time as has been found for the

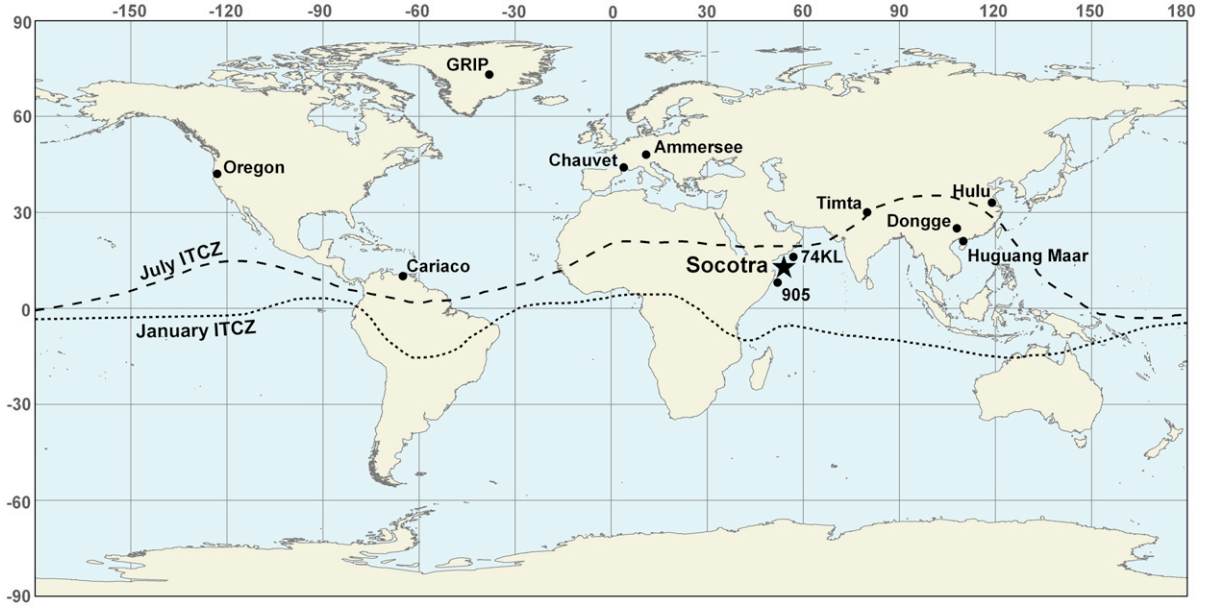

Fig. 1. Map showing the locations of the various records mentioned in the text as well as the modern position of the ITCZ during summer and winter (Lutgens and Tarbuck, 2001). Note the penetration of the ITCZ far into the Asian continent in the monsoon region during boreal summer. Socotra Island is in the northwest Indian Ocean and has a bimodal distribution of rainfall due to the migration of the ITCZ over the island in early summer and again in fall.

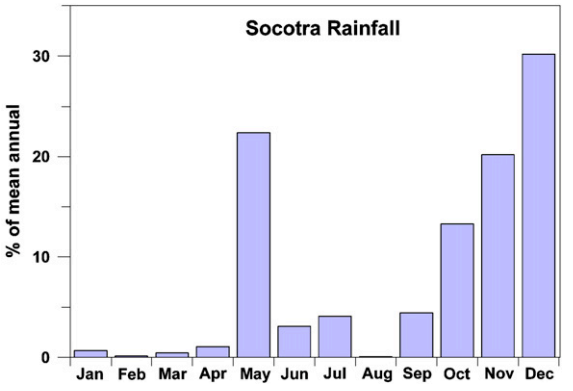

Fig. 2. Satellite derived rainfall data from NASA's Tropical Rainfall Measuring Mission (http://disc.sci.gsfc.nasa.gov/data/datapool/TRMM/01_Data_Products/02_Gridded/07_Monthly_Other_Data_Source_3B_43/index.html) from 1998–2006 centered at 12.375°N, 54.125°E with 0.25° resolution. Mean annual rainfall from this dataset is 100.3 mm.

Holocene (Dykoski et al., 2005; Fleitmann et al., 2003b; Wang et al., 2005; Neff et al., 2001).

Recent research has focused largely on understanding the nature and causes of the abrupt climate changes of the last deglaciation. While the relatively coarse resolution of most records has precluded detailed investigations into this subject, a growing body of well-dated, high-resolution records is being obtained through ice cores, varved sediments, and more recently speleothems. The sub-decadal resolution of these records can reveal the fine structure of abrupt climate changes. Furthermore, differences in the expression of rapid climate changes around the planet may allow pinpointing the 'epicenter' of these abrupt events, which would ultimately provide insights into the mechanisms responsible for them (Rodbell, 2000).

Researchers have also been concerned with identifying possible leads/lags between the tropics and high latitudes in order to better understand the relative role each plays in global climate change. Tropical speleothem records complement ice cores in this undertaking and may permit an assessment of the phasing of low and high latitude abrupt climate changes due to their good resolution and age control.

2. Location and modern climate

Socotra Island, Yemen lies in the northern tropics (12°30′ N 54° E) of the northwest Indian Ocean and is strongly influenced by the East African–Indian monsoon (Fig. 1) (Hastenrath, 1994; Webster et al., 1998; Fleitmann et al., 2007). The monsoon system has been viewed as both a large, seasonal scale land–sea breeze driven by ocean–continent thermal (and hence pressure) contrasts (Webster et al., 1998) and a manifestation of the annual migration of the intertropical convergence zone (ITCZ) into and out of southern Asia (Gadgil, 2003). The annual migration of the ITCZ in the Indian Ocean results in a bimodal distribution of rainfall on Socotra (Webster et al., 1998; Mies and Beyhl, 1996), delivering precipitation as it passes over the island in May–June and again from September–December (Fig. 2) (Fleitmann et al., 2007; Mies and Beyhl, 1996). Little to no rain falls on Socotra during the summer and winter monsoons; rather, the Arabian Sea region is dominated by the dry southwest (summer) and northeast (winter) trade winds (Webster et al., 1998; Fleitmann et al., 2007). Total annual rainfall on Socotra ranges from ~150 mm on the coastal plain to upwards of 500 mm in the interior mountains, which reach elevations >1000 m asl (Fig. 3) (Mies and Beyhl, 1996; Miller and Cope, 1996). Temperatures are warm with mean monthly values ranging from ~23.5–35 °C (Mies and Beyhl, 1996). The maritime climate of Socotra also maintains relatively high humidity, especially in comparison with the nearby desert regions of East Africa and the Arabian Peninsula (Mies and Beyhl, 1996). The reader is directed to Fleitmann et al. (2007) for a broader description of annual climate variability throughout the Indian Ocean region.

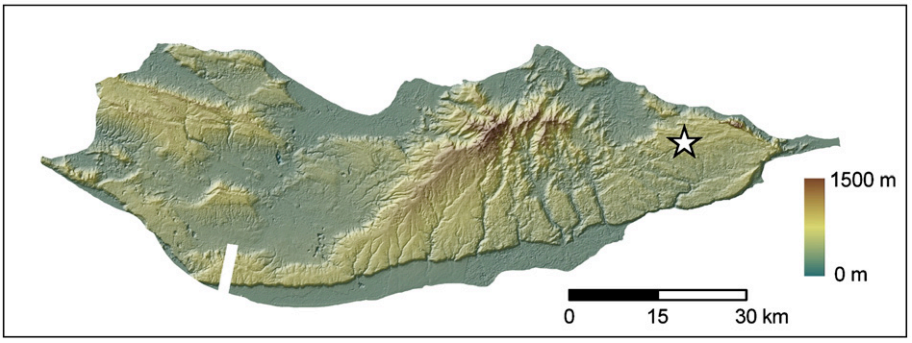

Fig. 3. Digital elevation model of Socotra Island derived from Advanced Spaceborne Thermal Emission and Reflection Radiometer (ASTER) data (http://elpdl03.cr.usgs.gov/pub/imswelcome/). Moomi Cave is represented by the white star.

3. Methods

3.1. Fieldwork and sample preparation

Stalagmite M1-5 (Fig. 4) was collected in 2002 from Moomi Cave, which lies on a carbonate plateau ~400 m asl on the eastern side of Socotra Island (Fig. 3). The cave is unmapped but initial exploration suggests it is >1 km in length, overlain by ~20 m of bedrock, quite horizontal, and has only one entrance. M1-5 was found standing nearly 1 km from the cave entrance; stalagmite M1-2 for reference, which was previously reported on by Burns et al. (2003), was collected ~200 m from the entrance. M1-5 was slabbed longitudinally along its growth axis and the interior surfaces were polished to make the internal stratigraphy more visible. The sample was investigated for signs of recrystallization and significant unconformities. A composite photograph was then taken of the speleothem (Fig. 4).

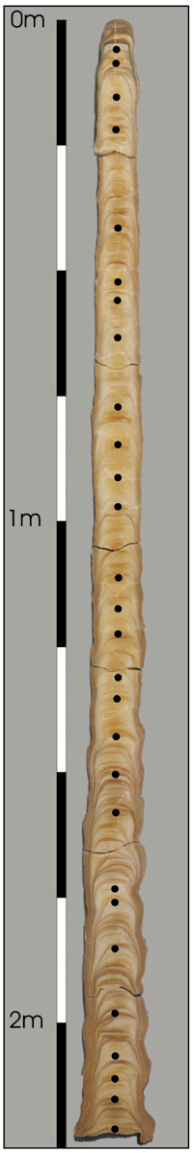

Fig. 4. Photograph of stalagmite M1-5. The black dots represent the locations of the 28 ^{230}Th dates obtained along the length of the speleothem. The speleothem's growth axis is remarkably straight and continuous and the sample grew quite rapidly. Color banding is quite prominent below 1.45 m depth, while variations in calcite appearance above this depth (except for the top 50 cm) are much smoother and less dramatic.

3.2. ^{230}Th dating

A drill corer was used to take a total of 28 ^{230}Th samples from M1-5 (Fig. 4), which were analyzed at the Isotope Geology Laboratory, University of Bern. Details of the chemical separation procedures and mass spectrometric measurements are given in Fleitmann et al. (2007).

3.3. Stable isotopes

Samples for stable isotope analysis were drilled along the growth axis using a 0.5 mm carbide dental burr. The speleothem slab was mounted on the stage of a Sherline micromill equipped with a digital tachometer (with 0.01 mm precision) to ensure accurate measurement of the sampling interval. Sample resolution is 1 mm for the top 0.122 m of the stalagmite, 2 mm from 0.122–0.272 m depth, and 4 mm from 0.272–2.224 m depth. 717 samples were taken in all. Ethanol was used to clean the speleothem surface and drill bit prior to sampling and they were brushed clean between samples.

The stable isotope samples were run on a Finnegan Delta XL ratio mass spectrometer coupled to an automated carbonate preparation system at the University of Massachusetts Stable Isotope Laboratory. Approximately 100 μg of powdered material was used per sample. Standard corrections for the phosphoric acid fractionation between calcite and CO_2, and for ^{17}O were applied to the results. Repeated analyses of an in-house standard indicate a within-run (40 samples plus 4 standards) reproducibility of 0.11 for δ^{18}O and 0.07 for δ^{13}C. All results are reported in parts per mil relative to the VPDB standard.

4. Results

4.1. Chronology

Ages of the 28 ^{230}Th measurements made on M1-5 range from 0.59–27.1 ka (Table 1). All ages are in

Table 1
Uranium-series dating results for stalagmite M1-5

Depth (mm)	U (ppb)	Th (ppb)	$^{234}U/^{238}U$	$^{230}Th/^{232}Th$	$^{230}Th/^{234}U$	Age (kyr before 1950 AD)
60	1122.454±2.888	0.797±0.005	0.9277±0.0012	23.17±0.66	0.0059±0.0002	0.588±0.015
88	1356.797±3.485	0.373±0.004	0.9345±0.0011	1000.09±13.93	0.0969±0.0007	11.086±0.122
155	1673.053±4.246	0.750±0.006	0.9558±0.0009	667.32±6.26	0.1034±0.0006	11.864±0.107
220	1970.127±5.000	0.333±0.002	0.9654±0.0007	1818.93±16.14	0.1044±0.0007	11.971±0.137
415	1493.490±3.784	1.102±0.011	0.9650±0.0006	448.61±5.09	0.1134±0.0007	13.085±0.137
525	1443.737±3.647	0.234±0.005	0.9729±0.0008	2145.24±53.09	0.1170±0.0011	13.558±0.183
562	1214.709±3.109	0.870±0.012	0.9722±0.0010	476.94±8.20	0.1161±0.0012	13.421±0.198
635	1587.156±4.031	0.154±0.002	0.9796±0.0007	3642.70±47.51	0.1172±0.0010	13.558±0.183
775	1937.116±4.961	0.575±0.036	0.9670±0.0008	1209.21±76.20	0.1223±0.0011	14.199±0.183
848	1967.268±4.974	0.578±0.003	0.9642±0.0006	1237.76±10.92	0.1242±0.0009	14.428±0.168
916	2135.293±5.454	2.637±0.050	0.9755±0.0012	298.26±5.93	0.1249±0.0007	14.534±0.122
973	2119.567±5.393	8.753±0.050	0.9787±0.0011	91.80±0.84	0.1283±0.0010	14.931±0.183
1115	2430.291±6.138	0.595±0.026	0.9801±0.0006	1658.50±73.45	0.1360±0.0012	15.908±0.214
1180	2147.513±5.443	2.490±0.022	0.9658±0.0006	343.80±4.19	0.1365±0.0012	15.999±0.214
1228	1393.028±3.537	0.120±0.001	0.9672±0.0009	4844.29±45.61	0.1395±0.0009	16.365±0.153
1314	2150.253±5.451	5.835±0.207	0.9598±0.0007	24.65±0.22	0.1418±0.0011	16.655±0.198
1355	2265.050±5.740	0.303±0.012	0.9503±0.0006	3208.73±130.53	0.1472±0.0011	17.342±0.214
1435	2246.824±5.676	5.591±0.030	0.9468±0.0006	172.73±1.33	0.1503±0.0009	17.739±0.183
1506	2449.744±6.192	0.383±0.002	0.9118±0.0006	2848.59±23.63	0.1593±0.0011	18.929±0.214
1581	2164.463±5.485	0.799±0.005	0.9178±0.0007	1228.43±11.19	0.1626±0.0011	19.371±0.198
1734	2706.921±6.837	1.987±0.014	0.8843±0.0006	633.64±6.04	0.1737±0.0012	20.852±0.229
1763	2379.473±6.008	4.160±0.148	0.8819±0.0006	266.22±9.63	0.1746±0.0012	20.974±0.244
1853	2392.214±6.064	1.187±0.009	0.8990±0.0006	1015.08±11.70	0.1846±0.0016	22.316±0.275
1983	2175.978±5.534	0.584±0.004	0.9356±0.0008	2114.25±19.26	0.1988±0.0014	24.208±0.275
2069	2447.538±6.172	1.083±0.006	0.9197±0.0006	1322.65±11.01	0.2094±0.0014	25.673±0.275
2115	2405.309±6.077	0.552±0.003	0.9170±0.0006	2598.78±21.66	0.2125±0.0013	26.131±0.244
2155	2062.966±5.243	4.017±0.048	0.9123±0.0008	310.96±4.25	0.2195±0.0016	27.108±0.305
2220	1906.123±4.812	7.645±0.040	0.9174±0.0006	150.17±1.15	0.2174±0.0013	26.802±0.275

All errors are 2σ.

stratigraphic order within 2σ analytical errors. Errors increase approximately linearly with age and vary from ~130 yr at 11 ka to ~290 yr at 27 ka. An age model was constructed by linearly interpolating between ^{230}Th dates and averaging dates where there are slight age reversals (at ~13.5 and 27.0 ka) (Fig. 5). The top date of 0.590 ka at 60 mm depth is separated from the next sample at 88 mm, which dates to 11.09 ka, by several rapid color changes and what appear to be corrosion surfaces. These features suggest a hiatus in deposition during most of the Holocene. Therefore, the uppermost age was not used in constructing the age model, and only isotopic data below the second date of 11.09 ka are discussed.

M1-5 appears to have been deposited under two different but fairly stable growth regimes. Growth rates were ~85 μm/yr from 27–17 ka and ~240 μm/yr from 17–11 ka and were relatively constant within each of these two time intervals. The mean growth rate over the length of the speleothem was 132 μm/yr. Stalagmite M1-2, also from Moomi Cave, grew from 53–40 ka at a fairly uniform rate along its entire length (Burns et al., 2003). Interestingly though, its mean growth rate was also 132 μm/yr.

4.2. Stable isotopes

Temporal sampling resolution of stable isotopes decreases nearly linearly from ~80 years at 27 ka to 10–20 years from 15–11 ka. $\delta^{18}O$ values (Fig. 6) range from −3.66 to 1.35‰ and average −1.41‰. From a multi-millennial perspective, $\delta^{18}O$ values increase almost 1‰ from the beginning of the M1-5 record at 27 ka to their peak at nearly 0‰ at ~23 ka. Oxygen isotopes then decrease irregularly until they reach their minimum of roughly −3.5‰ at approximately 14 ka. Thereafter, $\delta^{18}O$ increases steadily by ~2‰ until rapidly decreasing back to ~−3‰ at the end of the record at ~11.4 ka. Superimposed on these long-term changes are numerous, abrupt, decadal-scale shifts in $\delta^{18}O$. Prominent, rapid depletion events on the order of 1–2‰ are centered at 14.51, 11.40, and 11.24 ka and occur in a matter of decades. A major enrichment of ~1.5‰ occurs at 16.4 ka in roughly 50 yr.

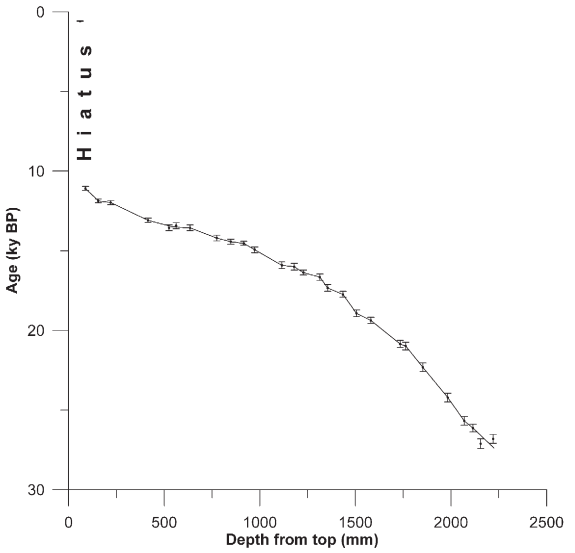

Fig. 5. Age versus depth plot for stalagmite M1-5. All ages are in stratigraphic order within the 2σ error bars. An age model was developed by linearly interpolating between data points and averaging dates where there are slight reversals (at ~550 and 2200 mm depth). Note that the top date occurred after a long period of non-deposition and was not included in the age model.

Two modern drip water samples from Moomi Cave have $\delta^{18}O$ values of −2.13 and −2.43‰ VSMOW. Given the current cave temperature of ~25 °C, modern calcite precipitated in equilibrium with these drips would have a $\delta^{18}O$ value of ~−4.3‰ VPBD. We unfortunately have no modern calcite from Moomi Cave, but this predicted value of −4.3‰ compares quite favorably with a late Holocene speleothem record from Dimarshim Cave on the western side of Socotra Island (Fleitmann et al., 2007).

5. Discussion

5.1. Equilibrium deposition?

A common concern in speleothem studies is whether calcite stable isotopes are a direct reflection of groundwater isotopes (Hendy, 1971; Harmon et al., 2004). There are two mechanisms that could potentially fractionate stable isotopes during speleothem deposition, in addition to the temperature-dependent fractionation inherent to calcite deposition from water. First, supersaturation of calcite in drip waters could be driven by evaporation, which occurs when cave humidity is less than 100% and fractionates oxygen isotopes by preferentially removing ^{16}O over ^{18}O (Hendy, 1971). Sample M1-5 was recovered, however, from the interior of Moomi Cave, nearly 1 km from the only known entrance, where evaporation should be minimal because of poor ventilation and thus high humidity values (Harmon et al., 2004).

Second, whereas the slow degassing of CO_2 from cave dripwaters maintains isotopic equilibrium among the various aqueous species, rapid CO_2 degassing does not permit the system enough time to equilibrate isotopically during deposition, fractionating carbon and oxygen isotopes (Hendy, 1971). Researchers often compare oxygen and carbon isotopes along the length of the speleothem growth axis to test for this kinetic effect as it fractionates both sets of isotopes in the same direction (i.e., toward heavier values) and thus causes them to covary.

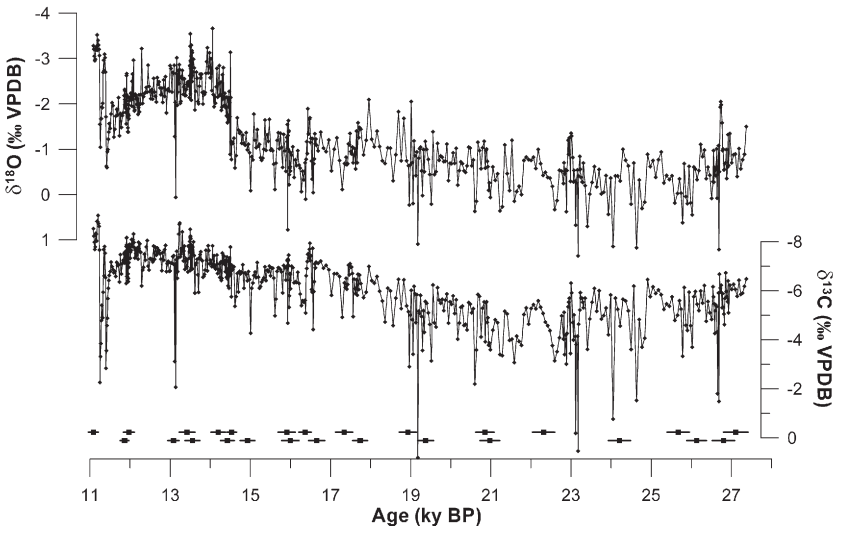

Fig. 6. The M1-5 $\delta^{18}O$ and $\delta^{13}C$ time series. ^{230}Th dates and 2σ error bars are shown on the bottom.

The fairly high correlation coefficient between carbon and oxygen isotopes over the entire length of the M1-5 record ($r^2=0.66$) and the similar structure of their decade to century-scale fluctuations prior to 16 ka suggest kinetic fractionation may have occurred. Furthermore, the visible stratigraphy shows a relatively large change in appearance at ~1.45 m depth (~18 ka), with considerably more pronounced layering and more frequent color changes below this depth, suggestive of more episodic or variable calcite deposition earlier in the record (Fig. 4). This may reflect less stable conditions earlier in the record during which evaporative or kinetic fractionation may have been more likely to occur. However, the much weaker correlation of the isotopes during the interval 14.6–11.1 ka ($r^2=0.39$) when the oxygen isotopes exhibit the greatest range of variation suggests a lesser role for kinetic effects in driving variability in this part of the record. The entire $\delta^{18}O$ record is characterized by considerable isotopic variability with at least a 0.5–1‰ shift occurring nearly every century. While it is uncertain if many of the excursions prior to 16 ka represent actual climate swings as opposed to kinetic effects since many are composed of only one or two data points, decadal to centennial-scale features in the younger part of the record consist of strings of data points and are not seen in the carbon isotopes indicating they are real climate events.

The striking degree of correspondence between M1-5 and the Dongge and Hulu Caves Chinese stalagmite records from 17–11 ka, discussed in detail below in Section 5.3, indirectly demonstrates that M1-5 faithfully tracked precipitation isotopes during at least this interval.

5.2. $\delta^{18}O$ interpretation

Before the M1-5 oxygen isotope record can be accurately interpreted in terms of climate, the various signals integrated in the $\delta^{18}O$ record must be separated. There are likely three main factors affecting the M1-5 $\delta^{18}O$ values. First, global ice volume affects the $\delta^{18}O$ of ocean water, and therefore precipitation, by storing relatively depleted water on land in the form of ice (Shackleton, 1967). This ice volume signal is also present in all other isotopic time series, precluding the need to extract it from paleoclimate records and facilitating their comparison; however, it should be quantitatively addressed to determine the proportion of isotopic variability attributable to non-ice volume effects. The $\delta^{18}O$ of seawater decreased ~1.0‰ from the Last Glacial Maximum (LGM) at ~21 ka to the present (Schrag et al., 1996). Assuming sea level and seawater $\delta^{18}O$ are linearly related, Dykoski et al. (Dykoski et al., 2005) determined that ocean $\delta^{18}O$ decreased ~0.15‰ before 16 ka and an additional ~0.35‰ from 16–11 ka, at which point the M1-5 record ends. Thus, this 0.5‰ shift due to ice volume effects accounts for ~15% of the ~3–3.5‰ absolute change seen in the running average of the M1-5 $\delta^{18}O$ record and helps explain slightly the long-term trend toward more depleted values in M1-5 after the LGM.

Second, the M1-5 $\delta^{18}O$ time series also likely reflects changes in cave temperature. The ~4‰ decrease observed in Socotra speleothem calcite $\delta^{18}O$ from the LGM to the present would imply a >15 °C glacial–interglacial warming if interpreted solely in terms of temperature, which is not plausible. Instead, sea surface temperatures (SSTs) in the tropical Indian Ocean increased ~2–3.5 °C from the LGM to the Holocene (Rostek et al., 1993; Emeis et al., 1995; Bard et al., 1997; Naidu and Malmgren, 2005), which is a reasonable estimate of changes in cave temperature during this interval due to the oceanic location of Socotra Island (Burns et al., 2003). Temperature changes of this magnitude would decrease speleothem $\delta^{18}O$ by ~0.44–0.77‰ due to calcite-water oxygen isotope fractionation (Harmon et al., 2004), explaining ~20% of the isotopic variability in M1-5.

Lastly, changes in the $\delta^{18}O$ of precipitation falling above the cave site exert a major control over speleothem $\delta^{18}O$. More specifically, this effect must account for approximately two-thirds of the isotopic variability in M1-5. Precipitation $\delta^{18}O$ on Socotra is likely a function of rainfall amount, with more negative values corresponding to greater rainfall and more positive values indicating decreased precipitation (Burns et al., 2003). Various lines of evidence support this interpretation. Numerous studies investigating isotopes in precipitation have found that rainfall amount and $\delta^{18}O$ are inversely correlated in the tropics due to an amount effect, with little or no observable correlation between temperature and precipitation isotopes (Dansgaard, 1964; Rozanski et al., 1993; Araguas-Araguas et al., 2000). Past research in Oman, nearly due north of Socotra, has inferred that the anticorrelation of calcite $\delta^{18}O$ and rainfall amount in the region has acted on 10^0–10^5 time scales, based on comparisons of speleothem $\delta^{18}O$ with modern instrumental data and other paleoclimate records of precipitation such as speleothem annual growth-layer thickness (Fleitmann et al., 2003a, 2004). Lastly, M1-5 and M1-2 (Burns et al., 2003), have more depleted (enriched) oxygen isotopes at times when other proxy records indicate increased (decreased) northern tropical rainfall and a stronger (weaker) monsoon (Schulz et al., 1998; Altabet et al., 2002; Wang et al., 2001; Dykoski et al., 2005; Peterson et al., 2000).

As mentioned above, rainfall is delivered to Socotra almost exclusively by the ITCZ. There are two ways in which this system could affect the $\delta^{18}O$ of precipitation

falling on Socotra. First, changes in the mean latitudinal position of the ITCZ could affect the seasonal duration and thus amount of rainfall experienced by the island. Second, changes in the intensity of convection of the ITCZ would alter the $\delta^{18}O$ of precipitation by affecting the proportion of moisture removed from the atmosphere via a Rayleigh distillation.

5.3. Comparison with other records

Burns et al. (Burns et al., 2003) found a relationship between Greenland and Socotra climate over Dansgaard/Oeschger (D/O) cycles 10–13 from 53–40 ka based on stalagmite M1-2, also from Moomi Cave, with a drier (wetter) Indian Ocean associated with North Atlantic stadials (interstadials). This teleconnection persisted through the end of the glacial period as demonstrated by the close correspondence between the M1-5 record and the Greenland ice cores (Fig. 7). Maximum aridity in Socotra occurs at ~23–24 ka, synchronous with peak LGM conditions in Greenland; an expression of H1 may be seen at ~16.4 ka as an abrupt drying and gradual wetting, similar to the structure of this event in the Hulu Cave East Asian monsoon record in eastern China (Wang et al., 2001); the B–A is a period of peak moisture in Socotra, followed by a gradual return to drier conditions during the YD; and rainfall increases abruptly at the onset of the Holocene at 11.4 ka. Centennial-scale events seen in the ice cores and the Cariaco Basin grayscale record (Hughen et al., 1996) during the B–A, such as the Intra-Bølling cold period, Older Dryas, and Intra-Allerød cold period, as well as the Preboreal Oscillation at ~11.2 ka, may have counterparts in M1-5 (Fig. 8), but this is difficult to evaluate with any certainty. There is also a major positive excursion in $\delta^{13}C$ associated with the Preboreal Oscillation. During the previous several thousand years $\delta^{13}C$ had been quite stable, raising the possibility that this event was exaggerated in M1-5 by isotopic disequilibrium effects. Given the fairly strong expression of D/O event 1 (the Bølling transition) as well as earlier millennial-scale D/O events in Socotra (Burns et al., 2003) it is reasonable to ask if the shorter lived D/O events nearer the glacial maximum were also felt there. The M1-5 record overlaps with D/O events 2 and possibly 3, which occur from ~23.4–23.1 and 27.8–27.5 ka in the new GICC05 chronology for the Greenland ice cores (Andersen et al., 2006). There are two depletion events seen in M1-5 $\delta^{18}O$ (but not $\delta^{13}C$) near 23.0 and 26.7 ka that may correlate with these D/O events, but this cannot be firmly established as they are fairly small in magnitude and little more than a century long. More data are needed to adequately address this issue, particularly since D/O event 3 may simply predate the M1-5 record.

Several recent studies have identified plausible mechanisms that could explain the observed North Atlantic–Indian Ocean teleconnection, from either the perspective of the Indian monsoon as an ITCZ phenomenon or as a large scale land–sea breeze. Modeling indicates increased Northern Hemisphere land and sea ice cover depresses the marine ITCZ southward [42,43]. Chiang and Bitz (Chiang and Bitz, 2005) attributed this

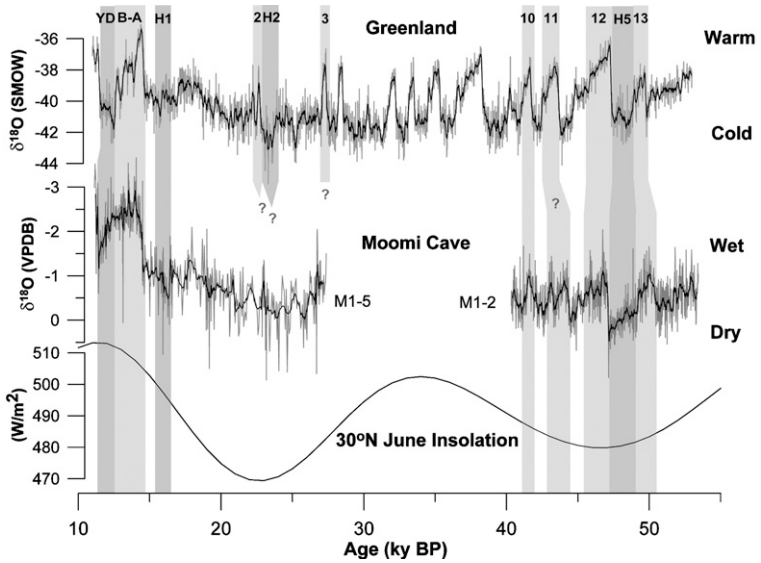

Fig. 7. Comparison of the Greenland ice core (Johnsen et al., 2001) and Moomi Cave, Socotra climate records. The M1-5 speleothem record is from this study and M1-2 is from (Burns et al., 2003). Dansgaard/Oeschger and Heinrich events are highlighted. Note the generally strong coupling of climate between these two regions over this time period. Insolation control on Socotra climate was strongly modulated by glacial boundary forcing.

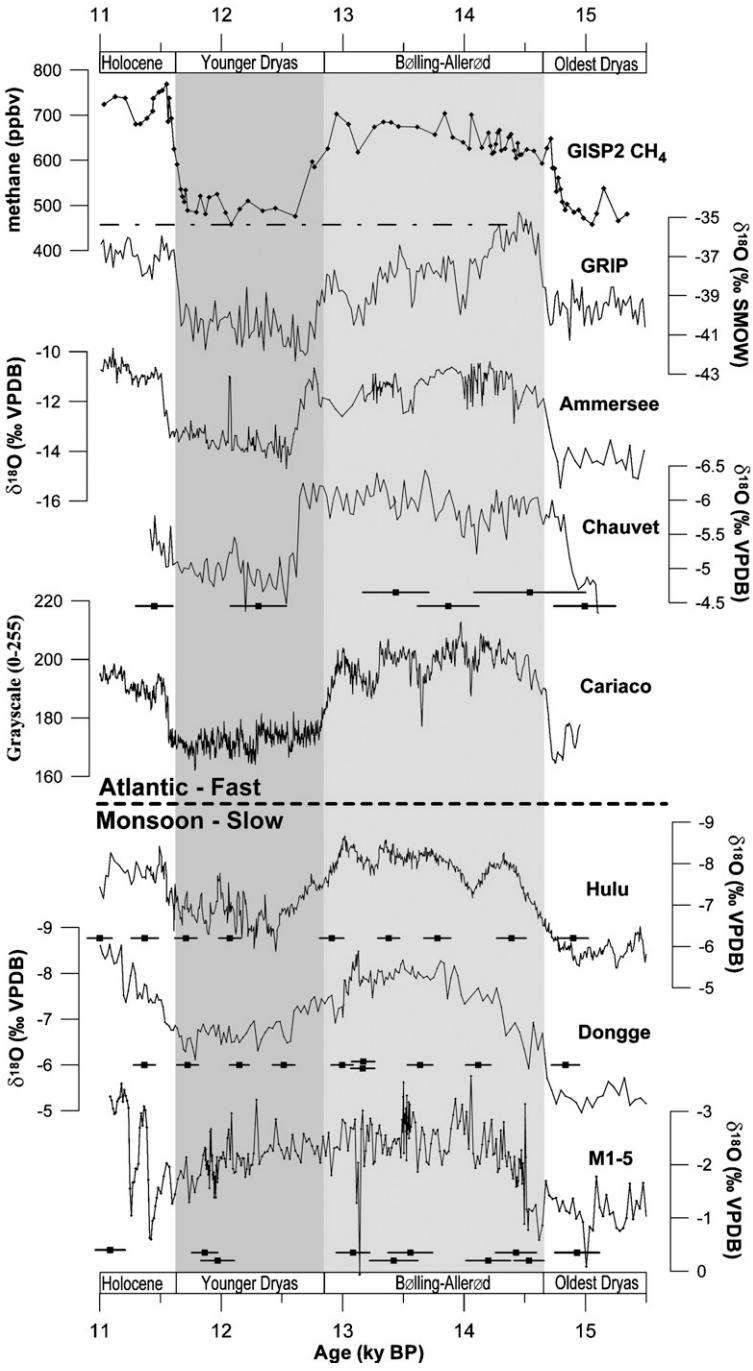

Fig. 8. Comparison of numerous high-resolution, deglacial climate records from the Northern Hemisphere. They are from top to bottom: GISP2 atmospheric methane concentrations (Blunier and Brook, 2001); Greenland ice core $\delta^{18}O$ (Rasmussen et al., 2006); Lake Ammersee, Germany $\delta^{18}O$ (von Grafenstein et al., 1999); Chauvet Cave, France $\delta^{18}O$ (Genty et al., 2006); Cariaco basin, Venezuala sediment grayscale values (Hughen et al., 1996); Hulu Cave, China $\delta^{18}O$ (Wang et al., 2001); Dongge Cave, China $\delta^{18}O$ (Dykoski et al., 2005); M1-5, Socotra Island $\delta^{18}O$ (this study). All records are plotted in thousands of years before 1950 AD. 2σ error bars on ^{230}Th dates are shown beneath each speleothem. The transitions into the Bølling and Younger Dryas are very abrupt in the four records from around the North Atlantic basin and atmospheric methane, but considerably more gradual in the cave records from the Asian monsoon region. This spatial pattern is consistent with a North Atlantic origin for these climate events.

effect to cooling of the northern extratropical atmosphere and ocean, which strengthens the northeast trade winds and leads to the southward propagation of a cold water front via a wind-evaporation-SST feedback. Once these cold waters reach the northern tropics they set up an anomalous pressure gradient that forces the ITCZ southward. Broccoli et al. (2006) similarly modeled a southward displacement of the ITCZ and strengthening of the northern Hadley cell when cooling the northern extratropics and warming the southern extratropics. The shift in tropical circulation helps compensate for the hemispherically asymmetric thermal forcing (Broccoli et al., 2006). Goswami et al. (2006) analyzed climate data from the last century and found that during strong phases of the North Atlantic Oscillation North Atlantic climate variability is effectively transferred to Eurasia via changes in winds and storm tracks. This atmospheric bridge can produce temperature anomalies in the middle and upper troposphere over Eurasia, which affects the duration of the summer monsoon by determining the length of time a positive tropospheric temperature gradient exists between the land and sea (Goswami et al., 2006).

A major difference between M1-5 and the Greenland ice cores is seen during the B–A. While Greenland $\delta^{18}O$ values begin to decrease from peak interstadial conditions immediately after the Bølling transition, M1-5 $\delta^{18}O$ values indicate a continued strengthening of the tropical hydrologic cycle into the Allerød period (Fig. 8). An upward slope or plateau during the B–A is also seen in many other records from the northern low to mid latitudes, including the Cariaco basin (Lea et al., 2003) and numerous speleothems from China (Wang et al., 2001; Dykoski et al., 2005; Zhao et al., 2003), India (Sinha et al., 2005), and the Mediterranean region (Genty et al., 2006). While Wang et al. (2001) suggested the speleothem and ice core records may be driven in different directions at this time due to decreasing ice volume, M1-5 $\delta^{18}O$ decreases by ~1‰ in the 500 yr after the Bølling transition, which is much too large to be explained by ice sheet melting. This trend is also present in ice core atmospheric methane records (Fig. 8), which is thought to largely be a proxy for the strength of the tropical hydrologic cycle during this time (Chappellaz et al., 1993; Brook et al., 2000). Furthermore, it is seen in speleothem $\delta^{13}C$ records from France, which are unaffected by ocean $\delta^{18}O$ (Genty et al., 2006). Thus, it seems likely low and northern high latitude climate evolved quite differently over the B–A. One possible explanation is that Northern Hemisphere ice cover retreated relatively slowly following the rapid increase in temperature recorded in Greenland ice (Dyke et al., 2003). The lag in ice retreat may have been expressed in the tropics as a slow continued strengthening of the monsoons and/or slow continued northward drift of the mean ITCZ location (Chiang et al., 2003). Alternatively, the position of the ITCZ is controlled by the interhemispheric temperature contrast and displaced toward the hemisphere with the lower pole-to-equator temperature gradient (Broccoli et al., 2006). Therefore, as the southern high latitudes cooled back into the Antarctic Cold Reversal during the B–A of the Northern Hemisphere, the ITCZ may have been forced slightly further north. Whatever the mechanism, it is worth mentioning that similar plateaus in tropical climate (Schulz et al., 1998; Altabet et al., 2002; Wang et al., 2001; Cai et al., 2006) and atmospheric methane records (Brook et al., 2000) are seen during some, but not all, earlier interstadials, even though Greenland immediately began cooling following every D/O event.

While insolation certainly represents a powerful forcing in the tropics, the M1-5 and M1-2 speleothem records from Socotra Island indicate that climate in the northern Indian Ocean was more strongly controlled by Northern Hemisphere ice volume and temperature forcing during the last glacial period, similar to the conclusions of other studies from the northwest Indian Ocean (Fig. 7) (Anderson and Prell, 1993; Fleitmann et al., 2003a; Overpeck et al., 1996; Burns et al., 2001).

A nearby Somali Margin $\delta^{15}N$ record of Arabian Sea denitrification (Ivanochko et al., 2005) displays a millennial-scale pattern of variability that is quite similar to the M1-5 time series (Fig. 9). As denitrification intensity in this region is ultimately driven by southwest monsoon wind-induced upwelling and productivity (Altabet et al., 2002; Ivanochko et al., 2005), a linkage between Indian monsoon wind strength and ITCZ mean location and/or convective intensity in the Indian Ocean is suggested. Core 74KL in the western Arabian sea provides further evidence of such a connection as it records abrupt increases in southwest monsoon winds at 16.0, 14.5, and 11.45 ka (Sirocko et al., 1996), synchronous with wetting events in M1-5 at the end of H1 and during the Bølling and Holocene transitions.

The D4 speleothem record from Dongge Cave in southeastern China overlaps with M1-5 from 16–11 ka. Oxygen isotopes in D4 are also thought to be driven by an amount effect and are interpreted to reflect changes in the strength of the Asian monsoon (Dykoski et al., 2005). In general, these two speleothem time series are remarkably similar (Fig. 8) despite the immense physical distance between them (~6000 km), which suggests both record a common signal — isotopes in precipitation driven by the strength of the Indian monsoon. Their overall millennial-scale structures are comparable and numerous decadal to centennial-scale events are likely correlative, most obviously the abrupt increase in monsoon strength at 14.6 ka

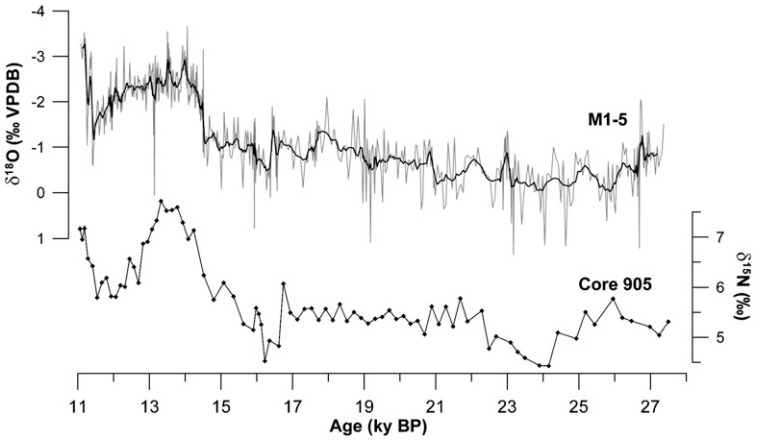

Fig. 9. Stalagmite M1-5 $\delta^{18}O$ versus Somali Margin core 905 $\delta^{15}N$ (Ivanochko et al., 2005), an indicator of Arabian Sea denitrification intensity. Denitrification in this region is controlled by productivity associated with southwest monsoon wind-induced upwelling. Therefore, the general similarity of M1-5 and core 905 suggests a relationship between the mean location and/or intensity of convection of the ITCZ in the Indian Ocean and Indian monsoon wind strength.

(Bølling transition) and the prominent dry event at 11.2 ka (Preboreal Oscillation). The similar timing of the events in these records, which are on independent time scales, reinforces the strength of their respective chronologies. Both exhibit a ~3‰ isotopic range from 11–16 ka, similar to the Hulu Cave record during this interval (Fig. 8). Also, the magnitudes of the transitions into the Bølling, the YD, and the Holocene are nearly identical in the speleothem records from these three caves, suggesting these climate events affected a large area of the monsoon region in the same way and to the same degree. Even more interesting, the structures of these climate changes are alike. In particular, the transitions into the Bølling period and the YD in all three records, as well as the Timta Cave record from northern India (Sinha et al., 2005), are remarkably gradual and take place over several centuries (Fig. 8). To be fair, there is a moderate jump in M1-5 $\delta^{18}O$ at the Bølling transition that is more or less pronounced depending on the age model we use; the ^{230}Th age control, however, precludes a clear, let alone abrupt, YD onset in M1-5. A relatively low-resolution speleothem record from Oregon, USA also shows a gradual YD transition (Vacco et al., 2005). The relatively gradual nature of these transitions is in striking contrast to their expression in the Greenland ice cores where they are very abrupt, occurring in only years to decades (Alley et al., 1993). These transitions are similarly rapid in other high-resolution archives from around the North Atlantic basin, such as the tropical Cariaco basin grayscale (Hughen et al., 1996) light color reflectance (Peterson et al., 2000), and SST (Lea et al., 2003) records, the Lake Ammersee, Germany $\delta^{18}O$ record (von Grafenstein et al., 1999), and speleothems from Chauvet Cave, southern France (Genty et al., 2006) (Fig. 8). At the other extreme, evidence for the B–A and YD oscillations in the southern mid-to-high latitudes is all together lacking or at best equivocal (Rodbell, 2000; Kaiser et al., 2005; Williams et al., 2005; Morgan et al., 2002).

A possible explanation as to why these climate shifts proceeded more slowly in the Indian Ocean–Asia region than in the North Atlantic is that the monsoon is largely driven by temperature contrasts between the Asian landmass and the southern Indian Ocean (Webster et al., 1998). Thus, these speleothem records may reflect, in addition to the primary northern high latitude signal, a secondary Southern Hemisphere temperature component (Cai et al., 2006). Moreover, modeling studies indicate anomalous meridional tropical SST gradients are essential to translating high latitude cooling into ITCZ displacement. Thus, the modeled ITCZ response to such a cooling tends to be less dramatic in continental settings and areas affected by complex monsoonal circulations (Chiang and Bitz, 2005; Broccoli et al., 2006), such as Socotra and the Asian cave sites discussed above. Additionally, the muted expression of the YD in Socotra may have been due to high summer insolation values dampening the effects of glacial boundary forcing at this time. The insolation maximum may have made the monsoon less "vulnerable" to the YD event. In any case, this spatially variable pattern of climate change is consistent with a North Atlantic origin for the B–A and YD climate events. Thus, high-resolution fingerprinting of these abrupt deglacial climate changes on land provides new evidence they were triggered by changes in the strength of thermohaline circulation and complements the paleoceanographic work on this subject (Hughen et al., 2000; McManus et al., 2004; Robinson et al., 2005).

For several reasons, we are confident that the gradual nature of these isotopic shifts are not inherent to speleothems as climate proxies or artifacts of data analyses, but instead accurately reflect the rate of climate change in the monsoon sector during the B–A and YD. Karst systems can respond quickly to climate change. For example, high amplitude, high frequency variability present elsewhere in the M1-5 record is abrupt in both directions, and abrupt changes are recorded in stalagmite M1-2 from the save cave (Burns et al., 2003). The onset of the Holocene, for example, occurs in ~30 years in M1-5 and <10 yr in Hulu Cave (Wang et al., 2001), and numerous rapid events are seen in the Dongge Cave record during the Holocene (Dykoski et al., 2005). Even more convincing, this pattern of climate change is replicated in five different caves from widely separated locations. Therefore, unless the age models of all of these records are incorrect, these signals of gradual deglacial climate changes are robust. Lastly, the onsets of the B–A and YD are very abrupt in stalagmites from southern France (Fig. 8) (Genty et al., 2006).

It should be mentioned that a new high-resolution record from Lake Huguang Maar in southeastern China shows a very abrupt YD onset in wind-delivered titanium concentrations (Yancheva et al., 2007). Age control here is considerably weaker than in the speleothem records making it difficult to definitively determine the structure of this event. If this transition truly was rapid at Lake Huguang Maar, however, it may point to differences in the seasonal expression of the YD (Denton et al., 2005) as this record is a winter monsoon proxy while the Asian speleothems record a summer monsoon signal.

Interestingly, ice core records indicate atmospheric methane concentrations changed rather abruptly during the Bølling and YD transitions (Fig. 8), more like North Atlantic climate than Asian monsoon strength. This observation may imply there were regions more important than the Asian monsoon sector in controlling atmospheric methane during the last deglaciation, perhaps areas more directly affected by Atlantic climate such as tropical South America (Lea et al., 2003; Maslin and Burns, 2000; Cruz et al., 2005) as has been suggested for the mid-Holocene (Koutavas et al., 2002). Indeed, Cariaco Basin biomarker records provide direct evidence for the rapid response of the tropical Atlantic terrestrial biosphere to the B–A and YD events showing vegetation there changed in near lock-step with North Atlantic climate with a lag of only decades (Hughen et al., 2004). Alternatively, if the Asian monsoon region was a significant player in deglacial methane fluctuations then it would appear that methane production there responds nonlinearly to climate change.

There has been considerable recent discussion of the phasing of low and high latitude climate change during glacial terminations. The lead of some tropical SST records and Andean deglaciation over global ice volume at the end of the last glacial period has been taken to suggest a tropical driver of climate change (Lea et al., 2000; Seltzer et al., 2002; Visser et al., 2003; Smith et al., 2005). However, the annually to decadally resolved records discussed above, which cover the northern low, middle, and high latitudes, do not support such an interpretation, at least on millennial time scales, because the start of major Northern Hemisphere warming, the Bølling transition, is synchronous within error in all of them at ~14.6 ka (Fig. 8) (Wang et al., 2001; Lea et al., 2003; Zhao et al., 2003). Also, the exact relationship between local marine $\delta^{18}O$ records and global sea level/ice volume remains uncertain (Clark and Mix, 2000; Skinner and Shackleton, 2005), limiting inferences of ice sheet mass balance based on tropical marine cores (Lea et al., 2000; Visser et al., 2003). It is possible that the inferred tropical temperature lead over northern high latitude ice volume is a function of the differing time constants involved in ocean warming, alpine glacier retreat, and ice sheet decay, and does not necessarily imply a tropical trigger for the climate changes of the last deglaciation.

6. Conclusions

Stalagmite M1-5 from Socotra Island provides the first high-resolution, absolute dated climate record over the last deglaciation from the western end of the Asian monsoon sector. The speleothem indicates Indian Ocean climate varied largely in concert with northern high latitude temperature being drier during stadial conditions and wetter during interstadials. Peak glacial dryness was reached at ~23 ka and followed by a gradual increase in moisture until an abrupt drying event at ~16.4 ka, which may correlate with Heinrich event 1. Rainfall increased abruptly at 14.51 ka synchronous with Bølling warming in Greenland. While Greenland immediately began cooling, however, Socotra continued to grow wetter into the Allerød. Thereafter, M1-5 records a gradual and continuous drying through the Allerød and Younger Dryas before rainfall increased abruptly at the onset of the Holocene at 11.40 ka. The Preboreal Oscillation is strongly expressed as a century-long dry event centered at 11.25 ka.

M1-5 is very well correlated with the Dongge Cave, China (Dykoski et al., 2005) record over the Bølling–Allerød and Younger Dryas, indicating these deglacial climate changes affected a wide area of the Indian Ocean monsoon region in the same manner. While the full transitions into the Bølling and Younger Dryas are very

abrupt in high-resolution records from around the Atlantic basin, they are quite gradual in M1-5 and all other Asian speleothem records. The differing structures of these climate events around the Northern Hemisphere suggest they originated in the Atlantic.

Acknowledgements

R. Soraruf provided valuable assistance in the UMass Stable Isotope Laboratory. We thank D. Sanz and M. A. Al-Aowah for help with sample collecting. Discussions with P. Clark were helpful. We are also grateful for the cooperation of the Environment Protection Authority, Socotra Island, Yemen, for permission to sample. I. Fairchild and two anonymous reviewers provided insightful comments that improved the original manuscript. This research was supported by the National Science Foundation (ATM-0135542).

Appendix A. Supplementary data

Supplementary data associated with this article can be found, in the online version, at doi:10.1016/j.epsl.2007.05.004.

References

Alley, R.B., Meese, D.A., Shuman, C.A., Gow, A.J., Taylor, K.C., Grootes, P.M., White, J.W.C., Ram, M., Waddington, E.D., Mayewski, P.A., Zielinski, G.A., 1993. Abrupt increase in Greenland snow accumulation at the end of the Younger Dryas event. Nature 362, 527–529.

Andersen, K.K., Svensson, A., Johnsen, S.J., Rasmussen, S.O., Bigler, M., Rothlisberger, R., Ruth, U., Siggaard-Andersen, M.-L., Peder Steffensen, J., Dahl-Jensen, D., Vinther, B.M., Clausen, H.B., 2006. The Greenland Ice Core Chronology 2005, 15–42 ka. Part 1: constructing the time scale. Quat. Sci. Rev. 25, 3246–3257.

Anderson, D.M., Prell, W.L., 1993. A 300 kyr record of upwelling off Oman during the late Quaternary: evidence of the Asian southwest monsoon. Paleoceanography 8, 193–208.

Altabet, M.A., Higginson, M.J., Murray, D.W., 2002. The effect of millennial-scale changes in Arabian Sea dentrification on atmospheric CO_2. Nature 415, 159–162.

Araguas-Araguas, L., Froehlich, K., Rozanski, K., 2000. Deuterium and oxygen-18 isotope composition of precipitation and atmospheric moisture. Hydrol. Process. 14, 1341–1355.

Bard, E., Rostek, F., Sonzogni, C., 1997. Interhemispheric synchrony of the last deglaciation inferred from alkenone paleothermometry. Nature 385, 707–710.

Blunier, T., Brook, E.J., 2001. Timing of millennial-scale climate change in Antarctica and Greenland during the last glacial period. Science 291, 109–112.

Broccoli, A.J., Dahl, K.A., Stouffer, R.F., 2006. Response of the ITCZ to Northern Hemisphere cooling. Geophys. Res. Lett. 33. doi:10.1029/2005GL024546.

Brook, E.J., Harder, S., Severinghaus, J., Steig, E.J., Sucher, C.M., 2000. On the origin and timing of rapid changes in atmospheric methane during the last glacial period. Glob. Biogeochem. Cycles 14, 559–572.

Burns, S.J., Fleitmann, D., Matter, A., Neff, U., Mangini, A., 2001. Speleothem evidence from Oman for continental pluvial events during interglacial periods. Geology 29, 623–626.

Burns, S.J., Fleitmann, D., Matter, A., Kramers, J., Al-Subbary, A., 2003. Indian Ocean climate and an absolute chronology over Dansgaard/Oeschger events 9 to 13. Science 301, 1365–1367.

Cai, Y., An, Z., Cheng, H., Edwards, R.L., Kelly, M.J., Liu, W., Wang, X., Shen, C.-C., 2006. High-resolution absolute-dated Indian Monsoon record between 53–36 ka from Xiaobailong Cave, southwestern China. Geology 34, 621–624.

Chappellaz, J., Blunier, T., Raynaud, D., Barnola, J.M., Schwander, J., Stauffer, B., 1993. Synchronous changes in atmospheric CH_4 Greenland climate between 40 and 8 kyr BP. Nature 366, 443–445.

Chiang, J.C.H, Bitz, C.M., 2005. Influence of high latitude ice cover on the marine Intertropical Convergence Zone. Clim. Dyn. 25, 477–496.

Chiang, J.C.H., Biasutti, M., Battisti, D.S., 2003. Sensitivity of the Atlantic Intertropical Convergence Zone to Last Glacial Maximum boundary conditions. Paleoceanography 18, 1094.

Clark, P.U., Mix, A.C., 2000. Ice sheet by volume. Nature 406, 689–690.

Clark, P.U., Alley, R.B., Pollard, D., 1999. Northern Hemisphere ice-sheet influences on global climate change. Science 286, 1104–1111.

Clemens, S., Prell, W., Murray, D., Shimmield, G., Weedon, G., 1991. Forcing mechanisms of the Indian Ocean monsoon. Nature 353, 720–725.

Cohmap, M., 1988. Climatic changes of the last 18,000 years: observations and model simulations. Science 241, 1043–1052.

Cruz Jr., F.W., Burns, S.J., Karmann, I., Sharp, W.D., Vuille, M., Cardoso, A.O., Ferrari, J.A., Silvia Dias, P.L., Viana Jr., O., 2005. Insolation-driven changes in atmospheric circulation over the past 116,000 years in subtropical Brazil. Nature 434, 63–66.

Dansgaard, W., 1964. Stable isotopes in precipitation. Tellus 16, 436–468.

Denton, G.H., Alley, R.B., Comer, G.C., Broecker, W.S., 2005. The role of seasonality in abrupt climate change. Quat. Sci. Rev. 24, 1159–1182.

Dyke, A.S., Moore, A., Robertson, L., 2003. Deglaciation of North America, Geol. Survery of Canada, Open File 1574 32 maps, 1:30,000,000.

Dykoski, C.A., Edwards, R.L., Cheng, H., Yuan, D., Cai, Y., Zhang, M., Lin, Y., Qing, J., An, Z., Revenaugh, J., 2005. A high-resolution absolute-dated Holocene and deglacial Asian monsoon record from Dongge Cave, China. Earth Planet. Sci. Lett. 233, 71–86.

Emeis, K.-C., Anderson, D.M., Doose, H., Kroon, H., Schulz-Bull, D., 1995. Sea-surface temperatures and the history of monsoon upwelling in the northwest Arabian Sea during the last 500,000 years. Quat. Res. 43, 355–361.

Fleitmann, D., Burns, S.J., Neff, U., Mangini, A., Matter, A., 2003a. Changing moisture sources over that last 330,000 years in northern Oman from fluid-inclusion evidence in speleothems. Quat. Res. 60, 223–232.

Fleitmann, D., Burns, S.J., Mudelsee, M., Neff, U., Kramers, J., Mangini, A., Matter, A., 2003b. Holocene forcing of the Indian Monsoon recorded in a stalagmite from southern Oman. Science 300, 1737–1739.

Fleitmann, D., Burns, S.J., Neff, U., Mudelsee, U.M., Mangini, A., Matter, A., 2004. Paleoclimatic interpretation of high-resolution oxygen isotope profiles derived from annually laminated speleothems from Southern Oman. Quat. Sci. Rev. 23, 935–945.

Fleitmann, D., Burns, S.J., Mangini, A., Mudelsee, M., Kramers, J., Villa, I., Neff, U., Al-Subbary, A.A., Buettner, A., Hippler, D., Matter, A., 2007. Holocene ITCZ and Indian monsoon dynamics recorded in stalagmites from Oman and Yemen (Socotra). Quat. Sci. Rev. 26, 170–188.

Gadgil, S., 2003. The Indian monsoon and its variability. Annu. Rev. Earth Planet. Sci. 31, 429–467.

Genty, D., Blamart, D., Ghaleb, B., Plagnes, V., Causse, Ch., Bakalowicz, M., Zouari, K., Chkir, N., Hellstrom, J., Wainer, K., Bourges, F., 2006. Timing and dynamics of the last deglaciation from European and North African $\delta^{13}C$ stalagmite profiles — comparison with Chinese and South Hemisphere stalagmites. Quat. Sci. Rev. 25, 2118–2142.

Global Demography Project; http://www.ncgia.ucsb.edu/pubs/gdp/.

Goswami, B.N., Madhusoodanan, M.S., Neema, C.P., Sengupta, D., 2006. A physical mechanism for the North Atlantic SST influence on the Indian summer monsoon. Geophys. Res. Lett. 33. doi:10.1029/2005GL024803.

Gupta, A.K., Anderson, D.M., Overpeck, J.T., 2003. Abrupt changes in the Asian southwest monsoon during the Holocene and their links to the North Atlantic Ocean. Nature 421, 354–356.

Harmon, R.S., Schwarz, H.P., Gascoyne, M., Hess, J.W., Ford, D.C., 2004. Paleoclimate information from speleothems: the present as guide to the past. In: Sasowsky, I.D., Mylroie, J. (Eds.), Studies of Cave Sediments. Kluwer Academic, New York, pp. 200–226.

Hastenrath, S., 1994. Climate Dynamics of the Tropics, vol. 8. Kluwer Academic Publishers, Boston.

Hendy, C.H., 1971. The isotopic geochemistry of speleothems-I. The calculation of the effects of different modes of formation on the isotopic composition of speleothems and their applicability as palaeoclimatic indicators. Geochim. Cosmochim. Acta 35, 801–824.

Hughen, K.A., Overpeck, J.T., Peterson, L.C., Trumbore, S., 1996. Rapid climate changes in the tropical Atlantic region during the last deglaciation. Nature 380, 51–54.

Hughen, K.A., Southon, J.R., Lehman, S.J., Overpeck, J.T., 2000. Synchronous radiocarbon and climate shifts during the last deglaciation. Science 290, 1951–1954.

Hughen, K.A., Eglinton, T.I., Xu, L., Makou, M., 2004. Abrupt tropical vegetation response to rapid climate changes. Science 304, 1955–1959.

Ivanochko, T.S., Ganeshram, R.S., Brummer, G.-J.A., Ganssen, G., Jung, S.J.A., Moreton, S.G., Kroon, D., 2005. Variations in tropical convection as an amplifier of global climate change at the millennial scale. Earth Planet. Sci. Lett. 235, 302–314.

Johnsen, S.J., Dahl-Jensen, D., Gundestrup, N., Steffensen, J.P., Clausen, H.B., Miller, H., Masson-Delmotte, V., Sveinbjšrndottir, A.E., White, J., 2001. Oxygen isotope and palaeotemperature records from six Greenland ice-core stations: Camp Century, Dye-3, GRIP, GISP2, Renland and NorthGRIP. J. Quat. Sci. 16, 299–307.

Kaiser, J., Lamy, F., Hebbeln, D., 2005. A 70-kyr sea surface temperature record off southern Chile (Ocean Drilling Program Site 1233). Paleoceanography 20. doi:10.1029/2005PA001146.

Koutavas, A., Lynch-Stieglitz, J., Marchitto Jr., T.M., Sachs, J.P., 2002. El Nino-like pattern in ice age tropical pacific sea surface temperature. Science 297, 226–230.

Lea, D.W., Pak, D.K., Spero, H.J., 2000. Climate impact of late Quaternary equatorial Pacific sea surface temperature variations. Science 289, 1719–1724.

Lea, D.W., Pak, D.K., Peterson, L.C., Hughen, K.A., 2003. Synchroneity of tropical and high-latitude Atlantic temperatures over the last glacial termination. Science 301, 1361–1364.

Lutgens, F.K., Tarbuck, E.J., 2001. The Atmosphereeighth ed. Prentice Hall, Englewood Cliffs.

Maslin, M.A., Burns, S.J., 2000. Reconstruction of Amazon Basin effective moisture availability over the past 14,000 years. Science 290, 2285–2287.

McManus, J.F., Francois, R., Gherardi, J.-M., Keigwin, L.D., Brown-Leger, S., 2004. Collapse and rapid resumption of Atlantic meridional circulation linked to deglacial climate changes. Nature 428, 834–837.

Mies, B.A., Beyhl, F.E., 1996. The vegetation ecology of Soqotra. In: Dumont, H.J. (Ed.), Proceedings of the First International Symposium on Soqotra Island: Present and Future. United Nations Publications, New York, pp. 35–82.

Miller, A.G., Cope, T.A., 1996. Flora of the Arabian Peninsula and Socotra. Edinburgh University Press, Edinburgh.

Morgan, V., Delmotte, M., van Ommen, T., Jouzel, J., Chappellaz, J., Woon, S., Masson-Delmotte, V., Raynaud, D., 2002. Relative timing of deglacial climate events in Antarctica and Greenland. Science 297, 1862–1864.

Naidu, P.D., Malmgren, B.A., 2005. Seasonal sea surface temperature contrast between the Holocene and last glacial period in the western Arabian Sea (Ocean Drilling Project Site 723A): Modulated by monsoon swelling. Paleoceanography 20, PA1004.

Neff, U., Burns, S.J., Mangini, A., Mudelsee, M., Fleitmann, D., Matter, A., 2001. Strong coherence between solar variability and the monsoon in Oman between 9 and 6 kyr ago. Nature 411, 290–293.

Overpeck, J., Anderson, D., Trumbore, S., Prell, W., 1996. The southwest Indian Monsoon over the last 18,000 years. Clim. Dyn. 12, 213–225.

Peterson, L.C., Haug, G.H., Hughen, K.A., Rohl, U., 2000. Rapid changes in the hydrologic cycle of the tropical Atlantic during the last glacial. Science 290, 1947–1951.

Rasmussen, S.O., Andersen, K.K., Svensson, A.M., Steffensen, J.P., Vinther, B.M., Clausen, H.B., Siggaard-Andersen, M.-L., Johnsen, S.J., Larsen, L.B., Dahl-Jensen, D., Bigler, M., Rothlisberger, B., Fischer, H., Goto-Azuma, K., Hansson, M.E., Ruth, U., 2006. A new Greenland ice core chronology for the last glacial termination. J. Geophys. Res. 111. doi:10.1029/2005JD006079.

Robinson, L.F., Adkins, J.F, Keigwin, L.D., Southon, J., Fernandez, D.P., Wang, S.-L., Scheirer, D.S., 2005. Radiocarbon variability in the western North Atlantic during the last deglaciation. Science 310, 1469–1473.

Rodbell, D.T., 2000. The Younger Dryas: cold, cold everywhere? Science 290, 285–286.

Rostek, F., Ruhland, G., Basslnot, F.C., Muller, P.J., Labeyrie, L., Lancelot, L., Bard, E., 1993. Reconstructing sea surface temperature and salinity using $\delta^{18}O$ and alkenone records. Nature 364, 319–321.

Rozanski, K., Auaguas-Araguas, L., Gonfiantini, R., 1993. Isotopic patterns in modern global precipitation. Geophys. Monogr. 78, 1–36.

Schulz, H., von Rad, U., Erienkeuser, H., 1998. Correlation between Arabian Sea and Greenland climate oscillations of the past 110,000 years. Nature 393, 54–57.

Schrag, D.P., Hampt, G., Murray, D., 1996. Pore fluid constraints on the temperature and oxygen isotopic composition of the glacial ocean. Science 272 (5270), 1930–1932.

Seltzer, G.O., Rodbell, D.T., Baker, P.A., Fritz, S.C., Tapia, P.M., Rowe, H.D., Dunbar, R.B., 2002. Early warming of tropical South America at the last glacial–interglacial transition. Science 296, 1685–1686.

Shackleton, N.J., 1967. Oxygen isotope analyses and Pleistocene temperatures re-assessed. Nature 215, 15–17.

Sinha, A., Cannariato, K.G., Stott, L.D., Li, H.-C., You, C.-F., Cheng, H., Edwards, R.L., Singh, I.B., 2005. Variability of southwest Indian summer monsoon precipitation during the Bølling–Allerød. Geology 33, 813–816.

Sirocko, F., Sarnthein, M., Erienkeusers, H., Lange, H., Arnold, M., Duplessy, J.C., 1993. Century-scale events in monsoonal climate over the past 24,000 years. Nature 364, 322–324.

Sirocko, F., Garbe-Schoenberg, D., McIntyre, A., Molfino, B., 1996. Teleconnections between the subtropical monsoons and high-latitude climate during the last deglaciation. Science 272, 526–529.

Skinner, L.C., Shackleton, N.J., 2005. An Atlantic lead over Pacific deep-water change across Termination I: implications for the application of the marine isotope stage stratigraphy. Quat. Sci. Rev. 24, 571–580.

Smith, J.A., Seltzer, G.O., Farber, D.L., Rodbell, D.T., Finkel, R.C., 2005. Early local last glacial maximum in the tropical Andes. Science 308, 678–681.

Vacco, D.A., Clark, P.U., Mix, A.C., Cheng, H., Edwards, R.L., 2005. A speleothem record of Younger Dryas cooling from the Klamath Mountains, Oregon. Quat. Res. 64, 249–256.

Visser, K., Thunell, R., Stott, L., 2003. Magnitude and timing of temperature change in the Indo-Pacific warm pool during deglaciation. Nature 421, 152–155.

von Grafenstein, U., Erlenkeuser, H., Brauer, A., Jouzel, J., Johnsen, S.J., 1999. A mid-European decadal isotope-climate record from 15,500 to 5000 years B.P. Science 284, 1654–1657.

Wang, Y.J., Cheng, H., Edwards, R.L., An, Z.S., Wu, J.Y., Shen, C.C., Dorale, J.A., 2001. A high resolution absolute-dated late Pleistocene monsoon record from Hulu Cave, China. Science 294, 2345–2348.

Wang, Y., Cheng, H., Edwards, R.L., He, Y., Kong, X., An, Z., Wu, J., Kelly, M.J., Dykoski, C.A., Li, X., 2005. The Holocene Asian monsoon: links to solar changes and North Atlantic climate. Science 308, 854–857.

Webster, P.J., Magana, V.O., Palmer, T.N., Shukla, J., Tomas, R.A., Yanai, M., Yasunari, T., 1998. Monsoons: processes, predictability, and the prospects for prediction. J. Geophys. Res. 103 (C7), 14451–14510.

Williams, P.W., King, D.N.T., Zhao, J.-X., Collerson, K.D., 2005. Late Pleistocene to Holocene composite speleothem ^{18}O and ^{13}C chronologies from South Island, New Zealand — did a global Younger Dryas really exist? Earth Planet Sci. Lett. 230, 301–317.

Yancheva, G., Nowaczyk, N.R., Mingram, J., Dulski, P., Schettler, G., Negendank, J.F.W., Liu, J., Sigman, D.M., Peterson, L.C., Haug, G.H., 2007. Influence of the intertropical convergence zone on the East Asian monsoon. Nature 445, 74–77.

Zhao, J.-X., Wang, Y., Collerson, K.D., Gagan, M.K., 2003. Speleothem U-series dating of semi-synchronous climate oscillations during the last deglaciation. Earth Planet. Sci. Lett. 216, 155–161.